

the signal is a bell-shaped curve and in the presence of saturation there is a dip at the line center (at $\omega \approx \omega_0$), the depth of the dip depending on the field amplitude H_1 . This is exactly the shape of the second harmonic signal which was observed in^[7].

There were three factors in^[7] which were ignored in our discussion and which could give rise to some discrepancies between the theory and experiment: 1) the field H_1 was applied in the form of pulses and, therefore, was not strictly speaking monochromatic; 2) we ignored the exchange interaction whose magnitude, for certain concentrations of the paramagnetic atoms, could be comparable with or even greater than the magnitude of the dipole-dipole interaction; 3) we ignored the inhomogeneous line broadening.

In conclusion, we shall point out that the functions $g(\Delta)$ and $g'(\Delta)$, as well as the functions $f(\omega_0 - 2\omega)$ and $f'(\omega_0 - 2\omega)$, satisfy the Kramers-Kronig relationships^[10] only approximately and only in the frequency range defined by $|\Delta| < (\sigma_0^2 + \omega_1^2)^{1/2}$ and $|\omega_0 - 2\omega| < \sigma_0$. This is due to the fact that the nature of these functions was reconstructed from the first three terms of their expansion as a power series in the operator V_t . One may expect that the retention of the higher terms in the expansion (5) will make it possible to describe higher-order nonlinear effects and to find more accurately the line profiles of the first and second harmonics by analogy with the refinement of the linear response profile obtained by inclusion of terms with higher powers of the dipole-dipole interaction operator.^[13]

The author is grateful to V. R. Nagibarov, N. K. Solovarov, and R. M. Yul'met'ev for their interest and comments.

- ¹B. N. Provotorov, Zh. Eksp. Teor. Fiz. **41**, 1582 (1961); **42**, 882 (1962) [Sov. Phys.-JETP **14**, 1126 (1962); **15**, 611 (1962)].
- ²M. Goldman, Spin Temperature and Nuclear Magnetic Resonance in Solids, Clarendon Press, Oxford, 1970 (Russ. Transl., Mir, M., 1972).
- ³V. A. Atsarkin and M. I. Rodak, Usp. Fiz. Nauk **107**, 3 (1972) [Sov. Phys.-Usp. **15**, 251 (1972)].
- ⁴A. G. Redfield, Phys. Rev. **98**, 1787 (1955).
- ⁵N. Bloembergen, Nonlinear Optics, Benjamin, New York, 1965 (Russ. Transl., Mir, M., 1966).
- ⁶R. Kubo and K. Tomita, J. Phys. Soc. Jpn. **9**, 888 (1954).
- ⁷R. Boscaino, I. Ciccarello, C. Cusumano, and M. W. P. Strandberg, Phys. Rev. B **3**, 2675 (1971); R. Boscaino, M. Brai, I. Ciccarello, and M. W. P. Strandberg, Phys. Rev. B **7**, 50 (1973).
- ⁸V. A. Atsarkin, Phys. Lett. A **48**, 485 (1974).
- ⁹I. K. Vagapov, Phys. Lett. A **51**, 255 (1975); I. K. Vagapov, Paper No. 1-75 deposited at VINITI, M., 1975.
- ¹⁰A. Abragam, The Principles of Nuclear Magnetism, Clarendon Press, Oxford, 1961 (Russ. Transl., IIL, M., 1963).
- ¹¹D. N. Zubarev, Neravnovesnaya statisticheskaya termodinamika, Nauka, M., 1971 (Nonequilibrium Statistical Thermodynamics, Vol. 1, Consultants Bureau, New York, 1974, Vol. 2—in preparation).
- ¹²L. L. Buishvili, Zh. Eksp. Teor. Fiz. **49**, 1868 (1965) [Sov. Phys.-JETP **22**, 1277 (1966)].
- ¹³Y. Doi and S. Aono, Prog. Theor. Phys. **51**, 1019 (1974).
- Translated by A. Tybulewicz

Domain structures of {111} iron garnet crystalline plates

G. S. Kandaurova and Yu. V. Ivanov

Ural State University, Sverdlovsk

(Submitted July 22, 1975)

Zh. Eksp. Teor. Fiz. **70**, 666-677 (February 1976)

The results are given of an investigation of the domain structure of {111} single-crystal iron garnet plates with a natural tetraaxial magnetocrystalline anisotropy. The domain structure was investigated with the aid of the Faraday effect. It was found that the structure was composed of three systems of through stripe domains oriented mainly along the $\langle 112 \rangle$ axis and forming a macrodomain structure. Several special features were observed in the behavior of this domain structure in a magnetic field, which was directed at right-angles or parallel to the plate. In particular, macrodomains without an internal substructure were observed during magnetization. The cause of the existence of an unusual hysteresis loop was established. Conditions were found under which the observed pattern became colored (the domains with different magnetization orientations had different "colors"). This effect was used in the identification of magnetic phases. A model of a complex domain structure was developed: it consisted of stripe domains with 71° walls and rhomboidal macrodomains with 109° walls, and the magnetization vectors of the domains were oriented along the $\langle 111 \rangle$ axes. The model described satisfactorily the magnetic-field-induced changes in the domain structure. The theoretically calculated relationships between the parameters of the macrodomain structure and stripe substructure were in agreement with the experimental results.

PACS numbers: 75.60.Fk, 75.50.Bb

New practical applications of magnetic domains demand a better understanding of the domain structure of ferromagnets and ferrimagnets (ferrites). The domain structure of magnetically uniaxial materials has been investigated in detail both theoretically and experi-

mentally, but much less work has been done on multi-axial crystals because of the greater variety of domain configurations which can occur in them. This applies particularly to the domain structure of magnetically multi-axial crystals with external surfaces which do not

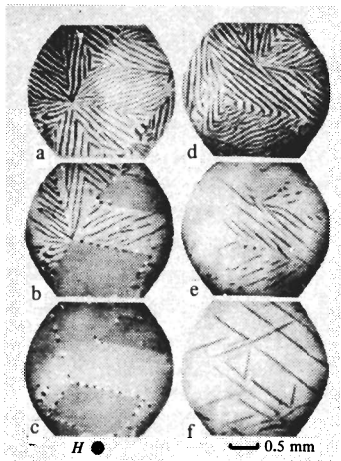


FIG. 1. Domain structure of an iron garnet crystal in various magnetic fields oriented perpendicular to the plane of the sample: a) 0; b) 21 Oe; c) 37 Oe; d) 69 Oe; e) 88 Oe; f) 83 Oe.

contain easy magnetization axes. In spite of the fact that the domain structure of multiaxial ferromagnets with cubic lattices has recently been the subject of very active research,^[1-10] the laws governing the formation of domain structures, relationship between different structures, and the nature of domain walls are far from fully understood. The best opportunities for the correct interpretation of domain structures and understanding of the mechanisms of changes in these structures in magnetic fields are available in the case of transparent crystals with a through structure which can be revealed by the Faraday effect. These crystals include sufficient thin iron garnet plates.

We investigated in detail the behavior of the domain structure of $(\text{Er}, \text{Tb}, \text{Gd})_3\text{Fe}_5\text{O}_{12}$ crystalline plates which were oriented nearly in the (111) plane (the deviation of the [111] axis from the normal did not exceed 5°); these plates were subjected to a magnetic field parallel or perpendicular to the plane of the sample. The plate thickness L was $\sim 60-80 \mu$. The observations were carried out both after careful mechanical polishing and after chemical polishing. Some laws governing the changes in the domain structure in magnetic fields were established for all the investigated samples. We shall illustrate them by considering a crystal of the specific composition $\text{Er}_{0.1}\text{Tb}_{0.5}\text{Gd}_{2.4}\text{Fe}_5\text{O}_{12}$ and 70μ thick.

1. DOMAIN STRUCTURE IN DEMAGNETIZED STATE

In the absence of a magnetic field the structure of the investigated composition consists of stripe domains oriented mainly along three directions coinciding with the (112) axes. The whole crystal splits into regions inside which the stripe domains are parallel to one another (Fig. 1a). This gives rise to a macrodomain structure^[4] with an internal fine substructure.¹⁾ In the general domain pattern there are sites from which stripe domains "emerge" and sites which are "bypassed" by stripe domains (we shall call them sites *A* and *B*, respectively). Two different sites of this kind can be seen in Fig. 1a.

Another feature of the domain structure is the sharp optical contrast of a boundary representing a wall between two neighboring stripe domains. Particles of a magnetic suspension deposited on the surface of a sam-

ple are precipitated at these boundaries. Consequently, the observed stripe domain structure can be regarded as a system of plane-parallel through layers with localized walls whose thickness is much less than the domain thickness. This structure is characterized by an open magnetic flux path and a distribution of magnetic charges on the surface in the form of stripes with alternate signs of the magnetic charge.

We shall assume that the magnetization vectors \mathbf{M} in stripe domains are parallel to the (111) axes (with the exception of the [111] axis). The walls between domains are parallel to the {110} planes. The question arises whether these are 180° or 71° walls. A calculation carried out for a Bloch wall shows that the surface energy density in the first case is^[12]

$$\gamma_{180} = 1.83 (AK)^{1/2}, \quad (1)$$

where A is the exchange interaction parameter and K is the first magnetic anisotropy constant; in the latter case,

$$\gamma_{71} = 1.22 (AK)^{1/2}. \quad (2)$$

Thus, the 71° Bloch walls are favored by energy considerations. However, the orientation of the magnetization in such a wall is close to the difficult direction. Therefore, we may expect the walls between these domains to be of the Néel rather than of the Bloch type. A calculation of the energy density in a 71° Néel wall gives the expression

$$\gamma_{71}^N = 2 \left(\frac{AK}{3} \right)^{1/2} \int_0^{\arccos \sqrt{2/3}} \{ 9 \cos^4 \varphi + 12 (\kappa - 1) \cos^2 \varphi + 8\sqrt{6} \kappa \cos \varphi + 4(1 + 2\kappa) \}^{1/2} d\varphi, \quad (3)$$

where $\kappa = 2\pi M^2/K$. The integral in Eq. (3) was calculated numerically for several values of κ . It was found that in the range $\kappa \leq 10$ this integral can be approximated by a quadratic trinomial and the energy (3) can be expressed analytically (to within 3%) in the form

$$\gamma_{71}^N \approx 0.46 (1 + 0.185\kappa - 0.006\kappa^2) (AK)^{1/2}. \quad (4)$$

We can see that in the case of iron garnets (typical values $\kappa \sim 1$) the energy of a 71° Néel wall is considerably lower than that of a corresponding Bloch wall.

Equation (4) allows us to estimate easily the domain thickness in the demagnetized state^[13]

$$d_0 = \frac{1.58}{M} [(1 + 0.185\kappa - 0.006\kappa^2) L \sqrt{AK}]^{1/2}. \quad (5)$$

Bearing in mind all the points made above, we can interpret the initial domain structure pattern, for example that near an *A* site, in the way it is done in Fig. 2b.

2. CHANGES IN DOMAIN STRUCTURE IN PERPENDICULAR MAGNETIC FIELD

When a crystal is magnetized in a perpendicular field, domain walls are displaced and stripes gradually

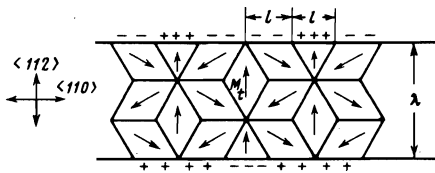


FIG. 4. Macrodomain structure model.

there be no magnetic charges on the walls is satisfied if the walls between the new domains and the matrix are parallel to the vectors \mathbf{M} in the macrodomains (Fig. 2c), i.e., if they are oriented at an angle 60° relative to the stripe domain walls in the initial magnetic state (Fig. 2d). Therefore, the type of site changes from A to B (compare Figs. 1a and 1d). The walls of the new stripe domains are the 71° Bloch walls, which are parallel to the $\{110\}$ planes. Theoretically, the energy of these walls is^[12]

$$\gamma_{71} = 0.46 (AK)^{1/2}. \quad (7)$$

They differ from the 71° walls separating stripe domains in the initial state in which the magnetization vectors in the domains have normal (to the wall) components amounting to $M \cos(\chi/2)$. In the case under discussion the magnetization rotates remaining all the time within the wall plane because if it were out of the plane the anisotropy energy as well as the exchange and magnetostatic energies would increase. Therefore, the energy described by Eq. (7) is smaller than that described by Eq. (4) and even smaller than the energy (2).

The normal (to the plane of the plate) components of the magnetization in neighboring stripe domains are, in accordance with the adopted model (Fig. 2d), M and $M \cos \chi$ and they are directed in the same way. Clearly, such a structure is equivalent to a Kittel structure^[13] in a crystal whose magnetization is $\frac{1}{2}(M - M \cos \chi)$, subjected to a magnetic field $H + H_m = H - 2\pi(M + M \cos \chi)$. In the pseudodemagnetized state the neighboring domains have the same thickness and, consequently, the average demagnetizing field H_m is compensated completely by the external field H . In this state the domain thickness may be expressed in the form

$$d_z = \frac{1.58}{M} (LVAK)^{1/2}, \quad (8)$$

which in the case of iron garnets with $\chi \sim 1$ is close to the domain width in the demagnetized state (5). A comparison of the domain structure photographs in Figs. 1a and 1d shows that this conclusion is in agreement with the experimental results.

3. MACRODOMAIN STRUCTURE MODEL

The appearance of macrodomains is due to the total magnetic moment of the stripe domain system parallel to the plane of the sample (Fig. 2b). Since the dimensions of a plate are finite, the existence of one stripe system, i.e., of one macrodomain, is not the preferred configuration. A reduction in the magnetostatic energy

is obtained when a macrodomain configuration is formed.

We shall consider the structure of macrodomains without a fine substructure (Fig. 1c). We shall assume that the plate is infinite in the $\langle 110 \rangle$ direction and that it can be regarded as ribbon of width λ . In this orientation one of the projections of the $\langle 111 \rangle$ axis, coinciding with $\langle 112 \rangle$, lies across the ribbon and the other two make angles of 30° and 150° with the edges. The proposed macrostructure model is shown in Fig. 4. It is selected on the basis of the following requirements: a) no charges on domain walls; b) zero total tangential component of the magnetic moment of the crystal. A characteristic feature of this structure is the possibility of variation in the number of rhomboidal domains across the width of the plate. The problem is to determine the equilibrium domain size l .

The energy of domain walls per unit length of the plate in such a structure is

$$E_w = \frac{2}{3} \gamma L \left(\frac{2\lambda}{\sqrt{3}l} - 1 \right). \quad (9)$$

We can calculate the magnetic energy by replacing the distribution of charges on the edge of the plate with a two-dimensional periodic structure comprising a set of the initial distributions separated by a distance T from one another (Fig. 5). Then, the magnetostatic energy per cell in such a structure can be expressed in the form

$$\epsilon_m = \frac{27M_t^2 l T}{8\pi^4} \sum_{n(\neq 0), p=-\infty}^{\infty} \frac{\sin^2(2\pi n/3) \sin^2(\pi p L/T)}{p^2 n^2 \sqrt{n^2/9l^2 + p^2/T^2}}, \quad (10)$$

where M_t is the tangential (with respect to the plane of the plate) component of the magnetization in the macrodomains. Going in Eq. (10) to the limit $T \rightarrow \infty$ and replacing summation over p with integration, we obtain the required magnetostatic energy of the edge charges. When this energy is recalculated per unit length of the plate, we obtain

$$E_m = \frac{81}{\pi^4} M_t^2 l \Sigma \left(\frac{L}{l} \right), \quad (11)$$

where

$$\Sigma(x) = \sum_{n=1}^{\infty} n^{-4} \sin^2 \left(\frac{2\pi n}{3} \right) \int_0^{\infty} \frac{\sin^2(\pi n x k/3)}{k^2 \sqrt{1+k^2}} dk. \quad (12)$$

In the range of small values of the ratio L/l ($0 < L/l$

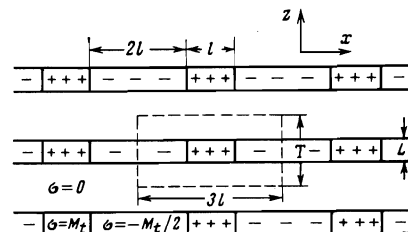


FIG. 5. Two-dimensional structure obtained by periodic repetition of a distribution of magnetic charges at the edge of a plate.



FIG. 6. Domain structure of an iron garnet crystal in various fields oriented parallel to the plane of the sample: a) 0; b) 4 Oe; c) 85 Oe; d) 0 Oe; e) -1 Oe.

< 0.5) the function $\Sigma(L/l)$ can be approximated by the polynomial

$$\Sigma(x) \approx P_3(x) = 0.11x + 2.44x^2 - 2.10x^3. \quad (13)$$

Then, Eq. (11) becomes

$$E_m = \frac{M_s^2 L}{\pi^2} \left\{ 8.9l + 198L - 170 \frac{L^2}{l} \right\}. \quad (14)$$

If we assume that l can vary continuously, we find that the condition

$$\frac{\partial}{\partial l} (E_m + E_w) = 0$$

can be used to find the equilibrium macrodomain size

$$l = 2.9(\gamma\lambda/M_s^2 - 2.27L^2)^{1/2}. \quad (15)$$

When the plate thickness L is increased, the value of l decreases rapidly and Eq. (15) is meaningful only if

$$L \leq 2.3(\lambda\gamma/4\pi M_s^2)^{1/2}. \quad (16)$$

When the above inequality is not satisfied, the ratio L/l lies outside the range of values in which the function $\Sigma(L/l)$ can be replaced by the polynomial (13). In the case of rare-earth iron garnets the characteristic length $\gamma/4\pi M_s^2$ is of the order of one micron and, therefore, in the case of plates with $\lambda \sim 1$ cm, the right-hand side of Eq. (16) represents hundredths of a centimeter. In the case of a sample whose domain structure is illustrated in Fig. 1, we have $L = 70 \mu$ and, therefore, the condition (16) is clearly satisfied; moreover, in rough estimates we can omit the second term from Eq. (15). Then, substituting in Eq. (15) the value of γ from Eq. (6) and $M_s = M \sin \chi \approx 0.94M$, we obtain the following

simple relationship between the macrodomain size l , thickness of stripe domains d_2 , and dimensions of the plate

$$l/d_2 \approx 2(\lambda/L)^{1/2}. \quad (17)$$

In our case ($L \sim 100 \mu$, $\lambda \sim 1$ cm), the stripe domain width should be approximately 20 times smaller than the macrodomain size. According to the experimental data, the above ratio is $l/d_{1,2} = 10-30$, which is in satisfactory agreement with the theoretical estimate.

4. CHANGES IN DOMAIN STRUCTURE IN PARALLEL MAGNETIC FIELD

The following changes in the domain structure occur when a field is applied parallel to the surface of the plate (Fig. 6). Even in weak fields $h \sim 0.05$ we find that instead of the three principal stripe domain systems there is only one dominant system in which the domain walls are oriented along the $\langle 112 \rangle$ axis, which makes the largest angle with the field H (Figs. 6a and 6b). When the field is increased, the macrodomains with this direction of the stripes grow and they absorb the neighboring regions. In fields $h > 0.1$ practically the whole crystal consists of just one system of stripe domains. When the field is reduced the stripe domains reappear and they are oriented along the same axis, their thickness increases, and in the residual magnetization state only one domain system remains in the sample (Fig. 6d). However, this domain structure is highly unstable. In negative fields $|h| > 0.01$ there is a sudden change in the domain structure: the macrodomain configuration is formed again (Fig. 6e) and magnetization continues in negative fields basically in the same way as in positive fields. Thus, the macrodomain structure exists only in a narrow range of fields near the demagnetized state. It should be noted that the hysteresis loop measured in the parallel field has the normal shape.

If the domain structure model shown in Figs. 2 and 4 is correct, the stripe domain walls (and, consequently, the vectors \mathbf{M}) should be oriented in the ideal case only along three directions in the plane of the plate. This means that discrete changes in the stripe domain positions may be expected when the field orientation is varied. In fact, it is found experimentally (Fig. 7) that rotation of the field in the plane of the sample produces one of these three "allowed" stripe domain systems. When the angle of rotation of the field φ is increased, the stripes retain their orientation and they switch suddenly to a new direction only when a certain critical value of the angle φ is reached. Figure 8 shows the dependence of the angle ψ , representing the dependence of the direction of the stripe domains in a crystal on the angle φ and it shows that the dependence $\psi(\varphi)$ is definitely step-like. The transition from one domain orientation to the other occurs in a very narrow range of angles.

5. COLORED DOMAIN STRUCTURE PATTERNS

The domain structure becomes colored when the laser source is replaced with white light and the polarizer

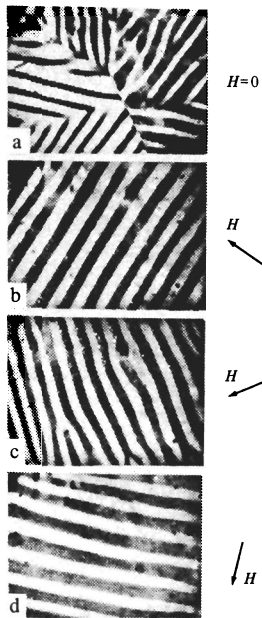


FIG. 7. Changes in the domain structure of the same sample as in Fig. 6 caused by changes in the field orientation.

and analyzer transmission axes have a certain relative orientation.^[14] The color of the domains depends strongly on the angle $\alpha = \pi/2 - \beta$, where β is the angle between the transmission axes. In the case of the sample whose domain structure is shown in Fig. 1, the maximum contrast between the domains and the strongest color effects are obtained for $\alpha = 3^\circ$ and $\alpha = -3^\circ$. The sequence of changes in the nature of the domain structure, domain color, and the presumed orientation of \mathbf{M} in domains are given in Table 1 for different magnetizing fields. If in the $\alpha = +3^\circ$ orientation a crystal is subjected to a negative field H , the domain pattern changes similarly to the case when $\alpha = -3^\circ$. If $\alpha = 0^\circ$, i.e., when the polarizer and analyzer transmission axes are completely crossed, all the domains are of gray-greenish color with domain boundaries appearing as dark thin lines.

When the crystal magnetization is switched by a perpendicular field, the sequence of appearance of domains of new color is in full agreement with the changes in the orientation of the domain magnetization deduced from the proposed model (Fig. 2). "Islands" of yellow or green color can frequently be seen against a background of a mass of "red" and "orange" domains. We may assume that when the field is switched off, the magnetic hysteresis maintains a residue of the magnetic phase with the same orientation of \mathbf{M} as in the state of

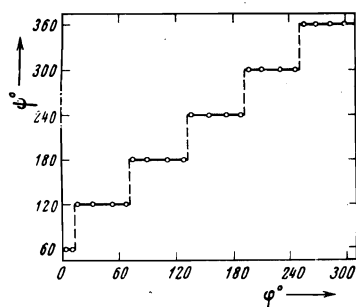


FIG. 8. Dependence of the the orientation of stripe domains ψ on the direction φ of the magnetic field.

TABLE 1. Relationship between observed domain color* and orientation of magnetization vectors.

State	$h = \frac{H}{H_s}$	Domain color		Orientation of \mathbf{M} in domains for $\mathbf{H} \parallel [111]$
		$\alpha = +3^\circ$	$\alpha = -3^\circ$	
Stripe domains (demagnetized state)	0	Orange	Red	$[\bar{1}\bar{1}1], [\bar{1}\bar{1}\bar{1}], [1\bar{1}\bar{1}]$
Macrodomains	0.3–0.5	Orange	Red	$[\bar{1}\bar{1}1], [1\bar{1}\bar{1}], [1\bar{1}\bar{1}]$
Stripe domains (pseudodemagnetized state)	0.7–0.8	Orange	Red	$[\bar{1}\bar{1}1], [1\bar{1}\bar{1}], [1\bar{1}\bar{1}]$
Single-domain state	1	Yellow	Green	$[111]$

*The observed colors are not spectroscopically pure. The domain color is given only approximately.

saturation in the fields $+H_s$ or $-H_s$, i.e., with \mathbf{M} directed along the $[111]$ or $[\bar{1}\bar{1}\bar{1}]$ axes. Since the color of each domain does not change when its volume is reduced or increased, we can assume that the rotation of \mathbf{M} in the domains during magnetization is of little importance and the main processes are the formation of nuclei of a new magnetic phase and the displacement of domain walls.

The appearance of colored domains may be attributed to the magnetic circular and linear dichroism, dispersion of the Faraday rotation, or magnetic birefringence.^[15–17] Clearly, further special studies would be needed to determine which of these factors predominates.

6. CONCLUSIONS

We investigated the domain structure of $\{111\}$ single-crystal iron garnet plates of different compositions. In all cases when an induced uniaxial anisotropy was not superimposed on the natural tetraaxial anisotropy, the equilibrium domain structure in the demagnetized state and the main features of the changes in the magnetic field were similar to those described above.

A comparison of the domain structure patterns revealed by powder and magneto-optic methods revealed that there were no closure domains in crystals 60–80 μ thick. The domain structure penetrated right through the plate. This made it easier to interpret it.

An analysis of the behavior of the domain structure in magnetic fields oriented in various ways relative to the crystallographic axis, together with x-ray diffraction data and results of studies of colored domain patterns, made it possible to construct models of the stripe and macrodomain structures which accounted for the observed features of the magnetic properties and domain structure such as the two-stage magnetization, unusual shape of the hysteresis loops, similar values of the stripe domain thickness in the demagnetized and pseudodemagnetized states, changes in the type of site, existence of macrodomains without an internal substructure in a perpendicular magnetic field, discrete changes of the stripe domain orientation in a parallel field, etc. Moreover, we were able to relate the macrodomain size to the dimensions of a crystal and to the stripe domain thickness. The agreement between

the theoretical estimates and experimental results confirmed once again the correctness of the selected models.

It can be shown that the general relationships governing the formation of the domain structure in {111} iron garnet plates apply also to other multiaxial ferromagnets with a similar magnetic anisotropy and comparable dimensions and crystallographic orientations of the samples. The domain structure can then be described by the theoretical representations put forward in the present paper.

It should be mentioned specially that the observation of colored domain structure patterns in which the color of a domain identifies the magnetic phase to which it belongs, opens up new possibilities for correct interpretation of the domain structure and identification of magnetic phases in magnetically multiaxial polydomain crystals. Clearly, a more careful analysis of the color patterns, carried out using special optical methods, may in future give much more extensive information on the distribution of the magnetization in domains and on the mechanism of changes in the domain structure than that obtained in the present study.

The authors are grateful to A. V. Andreev for an x-ray diffraction study of the crystals and to V. V. Zverev for his help in the investigation.

¹A macrodomain structure with a stripe substructure has been observed earlier in {100} single-crystal Mg-Mn ferrite films^{3,6,7} and in {100} nickel plates.¹¹

²The hysteresis loop was recorded using a Faraday hysteresis plotter when the angle between the transmission axes of the analyzer and polarizer was 45°.

- ¹V. K. Vlasko-Vlasov, L. M. Dedukh, and V. N. Nikitenko, Zh. Zh. Eksp. Teor. Fiz. 65, 377 (1973) [Sov. Phys.-JETP 38, 184 (1974)].
- ²R. V. Telesnin, L. I. Koshkin, T. I. Nestrelyaĭ, A. G. Shishkov, and N. A. Ékonomov, Fiz. Tverd. Tela (Leningrad) 13, 361 (1971) [Sov. Phys.-Solid State 13, 296 (1971)].
- ³T. I. Nestrelyaĭ and L. I. Koshkin, Sb. Magnetizm i Élektronika (Collection: Magnetism and Electronics), Kuibyshev, 1973, p. 18.
- ⁴N. A. Ékonomov and A. G. Shishkov, Fiz. Tverd. Tela (Leningrad) 16, 621 (1974) [Sov. Phys.-Solid State 16, 409 (1974)].
- ⁵R. V. Telesnin, E. N. Il'icheva, N. B. Shirokova, A. G. Shishkov, and N. A. Ékonomov, Kristallografiya 17, 566 (1972) [Sov. Phys.-Crystallogr. 17, 492 (1972)].
- ⁶L. I. Koshkin, T. I. Nestrelyaĭ, and T. A. Dunaeva-Mitlina, Fiz. Tverd. Tela (Leningrad) 11, 1216 (1969) [Sov. Phys.-Solid State 11, 987 (1969)].
- ⁷T. A. Dunaeva-Mitlina, Fiz. Tverd. Tela (Leningrad) 15, 3678 (1973) [Sov. Phys.-Solid State 15, 2449 (1974)].
- ⁸D. G. Berezin, T. A. Dunaeva-Mitlina, and B. V. Khramov, Fiz. Tverd. Tela (Leningrad) 15, 493 (1973) [Sov. Phys.-Solid State 15, 345 (1973)].
- ⁹T. R. Johansen, D. I. Norman, and E. J. Torok, J. Appl. Phys. 42, 1715 (1971).
- ¹⁰M. Dembinska, Acta Phys. Pol. A 45, 33 (1974).
- ¹¹P. W. De Blois, J. Appl. Phys. 36, 1647 (1965).
- ¹²A. Wachniewski, Acta Phys. Pol. 29, 437 (1966).
- ¹³C. Kittel, Phys. Rev. 70, 965 (1946).
- ¹⁴H. H. Schaum and A. Biehler, J. Sci. Soc. 3, 17 (1960).
- ¹⁵G. A. Smolenskii, R. V. Pisarev, I. G. Siniĭ, N. N. Kolpakova, and A. G. Titova, Izv. Akad. Nauk SSSR Ser. Fiz. 36 1219 (1972).
- ¹⁶G. A. Smolenskii, V. V. Lemanov, G. M. Nedlin, M. P. Petrov, and R. V. Pisarev, Fizika magnitnykh diélektrikov (Physics of Magnetic Insulators), Nauka, M., 1974.
- ¹⁷R. V. Pisarev, I. G. Siniĭ, and G. A. Smolenskii, Izv. Akad. Nauk SSSR Ser. Fiz. 34, 1032 (1970).

Translated by A. Tybulewicz

Phase transition in a nonequilibrium plasma and its effect on exciton condensation in germanium

B. M. Ashkinadze, N. N. Zinov'ev, and I. M. Fishman

A. F. Ioffe Physico-technical Institute, USSR Academy of Sciences
(Submitted August 1, 1975)
Zh. Eksp. Teor. Fiz. 70, 678-686 (February 1976)

Results are presented of an experimental investigation of recombination emission, absorption, and dispersion of microwaves in thin and bulky samples of pure germanium subjected to surface optical excitation. The results may be explained by means of an hypothesis that assumes the formation near the illuminated surface of the sample, of metastable dense plasma clusters that relax into electron-hole condensate drops.

PACS numbers: 72.30.+q

After L. V. Keldysh suggested in 1968 the possibility of the onset of electron-hole drops in semiconductors,^[1] a large number of experimental studies were made of this phenomenon (see, e.g.,^[2-6]). The results obtained to date allow us to conclude that at sufficiently low temperature the non-equilibrium excitons in germanium can condense into drops; the particle concentration in the

drops is $(2-3) \times 10^{17} \text{ cm}^{-3}$, and the temperature dependence of the dew point is extremely steep and corresponds to an activation energy $\approx 1.5 \text{ meV}$.^[4] Owing to the strong degeneracy ($E_F/kT \gg 1$), the electrons and holes in the drop have a high mobility corresponding to a relaxation time $\tau_r \sim 10^{-10} \text{ sec}$. The theoretical estimates of the particle concentration in the drop^[5] agree